THE ASTRONOMICAL JOURNAL VOLUME 104, NUMBER 6 DECEMBER 1992

NEAR-APHELION CCD PHOTOMETRY OF COMET P/SCHWASSMANN–WACHMANN 2[1]

J. X. LUU[2]

Harvard-Smithsonian Center for Astrophysics, 60 Garden Street, Cambridge, Massachusetts 02138

D. C. JEWITT

Institute for Astronomy, University of Hawaii, 2680 Woodlawn Drive, Honolulu, Hawaii 96822

Received 19 May 1992; revised 14 July 1992

ABSTRACT

We present CCD photometry of comet P/Schwassmann–Wachmann 2 obtained at 4.58 AU. The observations reveal cyclic variations in the comet brightness about a mean apparent red magnitude $m_R = 21.05 \pm 0.06$ mag and a range of approximately 0.5 mag. We find a best-fit lightcurve period $P_0 = 5.58 \pm 0.03$ h, which we interpret as the rotation period of the nucleus. No coma was seen in the individual exposures, but a faint coma extension toward the west was observed in a summed image. The derived upper limit to the radius of the nucleus is 3.1 km (assuming a value 0.04 for the geometric albedo). This renders Schwassmann–Wachmann 2 one of the smallest comet nuclei yet studied. The presence of cometary activity in Schwassmann–Wachmann 2 at a large heliocentric distance is consistent with the hypothesis of Rickman *et al.* [AJ, 102, 1446 (1991)] that comets new to the inner solar system possess relatively large free-sublimating areas on their surfaces.

1. INTRODUCTION

Comet P/Schwassmann–Wachmann 2 (hereafter SW2) was discovered in 1929, following a major perturbation of its orbit by Jupiter in 1926 (minimum separation 0.179 AU) (Marsden 1969). The perturbation resulted in its perihelion distance being reduced from $q = 3.56$ to $q = 2.09$ AU, and caused an increase in the orbital eccentricity (from $e = 0.1937$ to $e = 0.3946$). Dynamically, the interest in SW2 stems mostly from its strong transverse nongravitational acceleration A_2 (Marsden 1969; Marsden *et al.* 1973). The latter may imply a small nucleus radius and density, or an unusually large active area. Carusi *et al.* (1985) also identified SW2 as one of the comets that have been temporarily captured into satellite orbits of Jupiter. A handful of visual magnitudes were recorded in the IAU Circulars (e.g., Bortle 1979) during the 1979 apparition, but it has not so far been studied in detail using modern imaging technology. It was not favorably situated on its last apparition in 1987 and hence few observations were recorded at the time. As a result, very little is known about the physical properties of the comet. SW2 is presently on the inbound leg of its orbit and will reach perihelion again in 1994.

We observed SW2 as part of our ongoing program to identify and observe comet nuclei. Our scientific goal is to gather statistical information on this elusive group of objects and to ascertain their physical properties as a population. Most of the existing cometary database consists of observations of bright active comets whose nuclei are embedded within comae. Observations of bare comet nuclei are rare; the situation is reflected by the sample size of only a few studied nuclei (P/Halley, P/Arend–Rigaux, P/Neujmin 1, P/Tempel 2, P/Encke, and 2060 Chiron; see Belton 1991, Jewitt 1991, and references therein). Nuclei are typically visible in the absence of coma only when at large heliocentric distances (roughly $R > 4$ AU, where R is the heliocentric distance); at these distances, cometary activity decreases significantly or disappears altogether and the scattered light from the comet is dominated by the nucleus. Then, however, the observing task is frustrated by the small sizes of the nuclei (radius ~ 5 km) and their low albedos (~ 0.04) (A'Hearn 1988; Jewitt 1991). In our observing program, most of the nucleus observations were obtained when the comets were very faint (R magnitude ~ 19–21, e.g., this work). A complementary program of optical and infrared observations of near-Earth nuclei is being pursued by A'Hearn and his colleagues (e.g., A'Hearn *et al.* 1989; Millis *et al.* 1988).

To summarize, a successful attempt to observe a bare comet nucleus requires the identification of a comet in which the following balance is met: R has to be large enough so that the nucleus cross-section exceeds the combined cross-sections of the coma grains, yet R cannot be so large that the comet is too faint for observation. So far, the observed nucleus lightcurves have been found to have large amplitudes (Jewitt & Meech 1988; A'Hearn 1988). However, due to the small sample size, it is not clear if this characteristic is representative of all nuclei or is the result of observational selection. The sample size needs to be increased significantly before a rigorous statistical analysis of nucleus characteristics can be made.

In this paper we present charge-coupled device (CCD) photometry of comet SW2 at $R = 4.58$ AU, obtained shortly after it passed aphelion (at $Q = 4.82$ AU, in December 1990). Our observations span three nights in Sep-

[1]Observations taken at the Michigan–Dartmouth–MIT Observatory, operated by a consortium consisting of University of Michigan, Dartmouth College, and MIT.

[2]Current address: UC Berkeley, Dept. of Astronomy, 601 Campbell Hall, Berkeley, CA 94720.

 0004-6256/92/122243-07$00.90

TABLE 1. Viewing geometry of P/Schwassmann–Wachmann 2.

UT date	R [AU]	Δ [AU]	α [deg]	Scale [km/arcsec]
1991 Sep 12	4.585	3.674	5.97	2.67×10^3
1991 Sep 14	4.582	3.685	6.35	2.68×10^3
1991 Sep 15	4.581	3.692	6.56	2.69×10^3

tember 1991 and yield a lightcurve from which we infer the rotation period, an upper limit to the nucleus cross-section, and a lower limit to the equatorial axis ratio. We will present these results in the following sections and discuss the similarities and differences between SW2 and other well-studied comet nuclei.

2. OBSERVATIONS

Photometry of comet SW2 was obtained with a CCD on UT 1991 September 12, 14, and 15 with the 2.4 m telescope of the Michigan–Dartmouth–M.I.T. (MDM) Observatory on Kitt Peak, Arizona. The observations were made with the "Mark III" camera located at the telescope $f/7.5$ Cassegrain focus. The detector inside the camera was a 400 $\times$576 pixel Thomson CCD having 22 μm square pixels and a readout noise of 7 electrons. Used in conjunction with reimaging optics, the resulting image scale on the CCD was 0.73 arcsec/pixel. The telescope was tracked at sidereal rates at all times since the trailing of the comet during each integration (20.5″/hr or 2.1 arcsec in a 360 s exposure) was comparable to the seeing disk. All images were made in the Kitt Peak R filter (central wavelength $=6500$ Å, bandpass at full width at half maximum (FWHM) $=5800$–7200 Å) to exploit the high CCD efficiency in this wavelength range (NOAO Newsletter, Dec. 1989 issue).

The data analysis consisted of subtracting the bias from the images, and then dividing the bias-subtracted images by a "flat field" to remove pixel-to-pixel sensitivity variations. The bias for each image was obtained by measuring the overclock region, while the flat field was a median-filtered image of many ($\sim$15) images of the twilight sky. The resulting "flattened" images were found to be uniform to $\sim$0.5% across the width of the chip. At this level, the errors introduced by the nonuniform sensitivities of the pixels are negligible compared to the uncertainties in the photometry of comet SW2 itself. For flux calibration purposes, images of Christian standard star fields (Christian *et al.* 1985) were taken several times throughout each night. The extinction coefficient for each night was determined from field stars in the comet images, and verified by observing the same standard fields at different airmasses. The viewing geometry of SW2 at the time of the observations is summarized in Table 1.

Successive images of the comet were taken under photometric conditions on three nights, with 1.5″–2″ FWHM seeing on all nights. The comet appeared at the ephemeris position and was moving in the expected direction at the expected rate, precluding confusion with field asteroids. A 3-pixel radius (2.2″) circular diaphragm was used for the photometry. The background sky was measured in an annulus 10 pixels (7.3″) in width and 5 pixels (3.7″) in inner radius. The resulting error in the photometry was approximately $\pm$5%–7%, stemming mostly from the uncertainties in measuring the sky.

TABLE 2. CCD Photometry of P/Schwassmann–Wachmann 2.

UT date	UT start time	$m_R\pm\sigma_{m_R}$[1]	Airmass
1991 Sep 12	7.7369	20.91±0.06	1.818
1991 Sep 12	7.8278	20.73±0.06	1.851
1991 Sep 12	7.9200	20.93±0.06	1.887
1991 Sep 14	3.3933	20.87±0.06	1.834
1991 Sep 14	5.3567	21.31±0.06	1.796
1991 Sep 14	5.4453	21.21±0.06	1.496
1991 Sep 14	5.7239	21.02±0.06	1.499
1991 Sep 14	5.8300	20.93±0.06	1.502
1991 Sep 14	6.0431	20.91±0.06	1.514
1991 Sep 14	6.3803	21.05±0.06	1.545
1991 Sep 14	6.4897	20.90±0.06	1.559
1991 Sep 14	6.8208	21.08±0.06	1.612
1991 Sep 14	6.9275	21.07±0.06	1.633
1991 Sep 14	7.0342	20.97±0.06	1.656
1991 Sep 14	7.1419	21.06±0.06	1.682
1991 Sep 14	7.5742	21.17±0.06	1.814
1991 Sep 14	7.8978	21.10±0.06	1.949
1991 Sep 14	8.1269	21.14±0.06	2.069
1991 Sep 15	2.6589	20.66±0.06	2.171
1991 Sep 15	2.7511	20.86±0.06	2.107
1991 Sep 15	2.8736	21.11±0.06	2.033
1991 Sep 15	2.9797	21.08±0.06	1.978
1991 Sep 15	3.2075	21.00±0.06	1.873
1991 Sep 15	3.4228	21.25±0.06	1.792
1991 Sep 15	3.5444	21.30±0.06	1.752
1991 Sep 15	3.8736	21.28±0.06	1.663
1991 Sep 15	4.0914	21.19±0.07	1.617
1991 Sep 15	4.3464	20.99±0.07	1.574
1991 Sep 15	4.4567	20.94±0.07	1.559
1991 Sep 15	4.5647	21.13±0.07	1.545
1991 Sep 15	4.7867	21.02±0.07	1.523
1991 Sep 15	5.4403	20.95±0.07	1.497
1991 Sep 15	5.5469	20.91±0.07	1.498
1991 Sep 15	5.6542	21.00±0.05	1.500
1991 Sep 15	5.7625	21.01±0.05	1.504
1991 Sep 15	5.8700	21.07±0.05	1.509
1991 Sep 15	5.9917	21.14±0.05	1.517
1991 Sep 15	6.0989	21.14±0.05	1.529
1991 Sep 15	6.2108	21.10±0.05	1.536
1991 Sep 15	6.3200	20.97±0.05	1.548
1991 Sep 15	6.4275	21.07±0.05	1.562
1991 Sep 15	6.7519	21.04±0.05	1.614
1991 Sep 15	6.8586	21.02±0.05	1.635
1991 Sep 15	6.9794	20.99±0.05	1.662
1991 Sep 15	7.1953	21.00±0.05	1.718
1991 Sep 15	7.3031	20.95±0.05	1.750
1991 Sep 15	7.4097	21.02±0.06	1.783
1991 Sep 15	7.5164	20.76±0.06	1.821
1991 Sep 15	7.6244	20.84±0.06	1.863

[1]Magnitudes have been corrected for airmass.

3. DISCUSSION

3.1 Rotation Period

A summary of the SW2 photometry is provided in Table 2. In all individual images, the comet appeared stellar, with

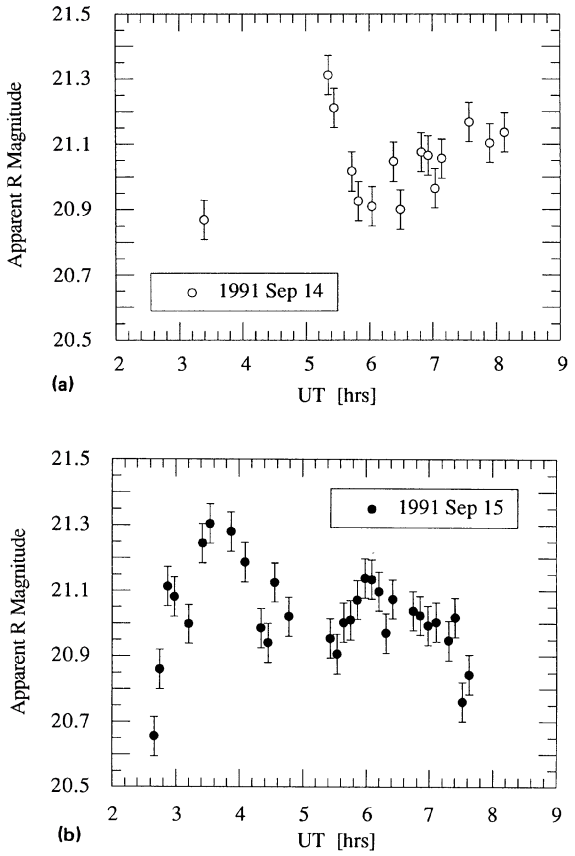

FIG. 1. *R*-filter photometry of SW2 over two nights, with the apparent magnitude plotted as a function of time. (a) 14 September 1991, (b) 15 September 1991.

no apparent coma (although a coma extension could be seen when all the images were added together—see Sec. *3.2*). When plotted as a function of time, as in Fig. 1, the apparent brightness of the comet showed nonrandom variations about a mean red magnitude $\overline{m_R} = 21.05 \pm 0.06$, with a range as large as $\Delta m = 0.5 \pm 0.1$. The magnitude of the comet reduced to $R = \Delta = 1$ AU and 0° phase angle [denoted by m (1,1,0)] can be estimated from

$$m_R(1,1,0) = m_R - 5\log(R\Delta) - \beta\alpha, \quad (1)$$

where β is the linear phase coefficient and α is the phase angle. Assuming an empirical phase coefficient $\beta = 0.04$ mag/deg (as is typical for other known nuclei, e.g., P/Encke, Luu & Jewitt 1990; P/Tempel 2, Sekanina 1976, Jewitt & Luu 1989), we find that SW2 in September 1991 has the absolute red magnitude

$$m_R(1,1,0) = 14.64 \pm 0.06. \quad (2)$$

The photometry plotted in Fig. 1(b) shows two maxima and two minima in an observing window of ~5.5 h, suggestive of a rotating nucleus. We searched for periodicity in the combined photometry by applying a phase dispersion minimization method (e.g., see Dworetsky 1983) to the data. The search yielded a best-fit period at $P_0 = 5.58 \pm 0.03$ h. The uncertainty was estimated from the results of the phase dispersion minimization method and from phase plots constructed with other periods. Figure 2 shows the photometry as a function of rotational phase assuming the 5.58 h period, while Fig. 3 shows the phase plots for the periods 5.49 h ($P_0 - 3\sigma$) and 5.67 h ($P_0 + 3\sigma$). As the viewing geometry remains essentially unchanged over the observing period (see Table 1), the apparent brightness of the comet on all nights is plotted.

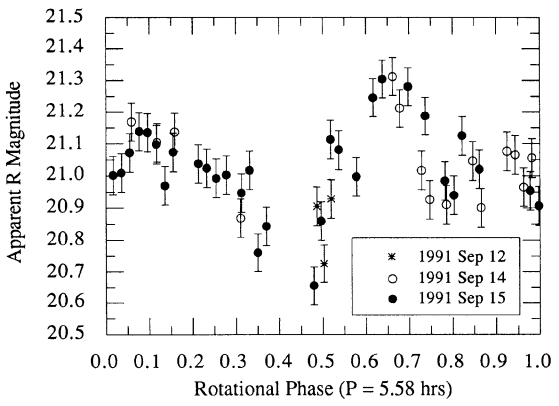

FIG. 2. Rotational phase plot of SW2 using the best-fit period $P_0 = 5.58$ h. It shows two maxima per period, as expected from a lightcurve produced by the rotation of an aspherical body.

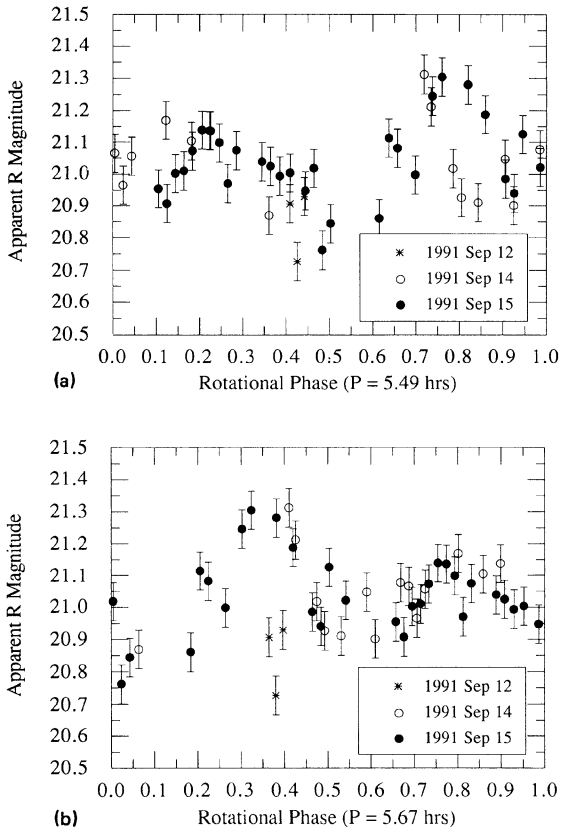

FIG. 3. Rotational phase plot of SW2 using (a) $P_0 - 3\sigma = 5.49$ h and (b) $P_0 + 3\sigma = 5.67$ h. Both plots show poor correlation in the brightness variations.

The shape of the lightcurve may be caused by rotation of a highly aspherical nucleus, the presence of high albedo spots rotating past the line of sight, or by a periodically modulated coma. However, the large asymmetry between the two maxima precludes the possibility that the period is $P_0/2$ and caused by a single high albedo spot. The possibility of two albedo spots cannot be excluded using optical data alone, but by analogy with other cometary nuclei observed simultaneously in the optical and infrared (e.g., Millis *et al.* 1988; A'Hearn *et al.* 1989) we favor the hypothesis of a rotating aspherical nucleus (see Sec. *3.3* below).

The tangential nongravitational parameter A_2 is traditionally attributed to the deviation of reaction forces away from the Sun–comet line due to a coupling of the nuclear spin and outgassing activities at the nucleus surface (Marsden 1969; Belton 1991). Large negative values for A_2 imply that the comet is subjected to large secular acceleration (Marsden 1969), and increase the possibility of precession. Within the photometric uncertainties, we find no evidence for precession in the presented lightcurve. However, it is possible that precession exists on a time scale longer than can be detected during three nights of observation. Further observations of SW2 during its approach to perihelion are warranted and highly encouraged as it presents a prime candidate for precession induced by nongravitational forces.

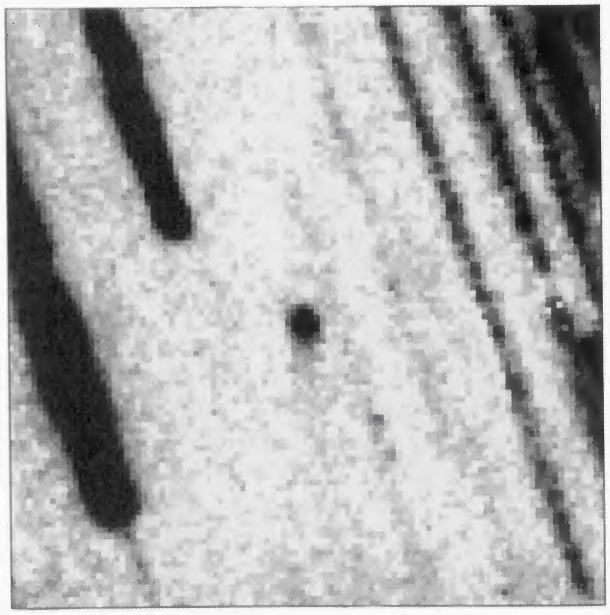

FIG. 4. The sum of 48 individual images of SW2, with an effective integration time of 4.8 h. The comet is in the center and the stars appear in lines because the images have been shifted to cancel out the motion of the comet. The dimensions of the image are 75″×75″; North is to the left, and West is toward the bottom. A very faint extension is visible directly below the comet (position angle ~270°±5°).

3.2 Cometary Activity?

No coma was apparent in the individual 360 s integrations. Nevertheless, we searched for the presence of very faint near-nucleus coma by adding all images together to produce a single deep image. The summed image has an effective integration time of 17280 s (4.8 h); a portion of the image (dimensions ~75″×75″) centered on SW2 is shown in Fig. 4. The individual images which make up Fig. 4 have been shifted to cancel out the motion of SW2, causing field stars to appear in straight lines. The deep image in Fig. 4 shows that the comet exhibits a coma extending toward the west.

We further examine the nature of SW2's coma by means of surface brightness profiles. Figure 5 shows the profile of the comet, obtained by plotting the intensity perpendicular to the projected motion of the comet, along with the profile of a field star. The figure shows that the SW2 profile is very similar to that of the star, implying that the comet is unresolved in the direction perpendicular to the projected motion, and that the coma is only resolved roughly in the direction of motion (west direction). The westward extension (position angle ~270°±5°) does not coincide with the antisolar direction (position angle ~111°), and thus is not the radiation pressure-induced "tail" found in many comets. Instead, we found that the extension better coincided with the orbital plane of the comet (position angle ~258°), and could be explained by ejected particles which co-orbit with the comet. If the extension were caused by co-moving grains, this would eliminate the requirement that SW2 was active at the time of observation, since the grains could have been ejected during a different portion of the orbit. We have no constraint on when the co-moving grains were ejected and hence how recent was the cometary activity.

The surface brightness $\Sigma(r)$ of the coma extension (at $r\sim2''$ from the nucleus) was about 0.3% of the sky background, or $\Sigma(r)\sim27.3$ mag/sq.arcsec. If the unresolved coma had a symmetric $1/r$ dependence, then an upper limit to the integrated magnitude within a 2.2″ radius aperture, m_{coma}, can be found from the surface brightness via the equation (Jewitt 1991)

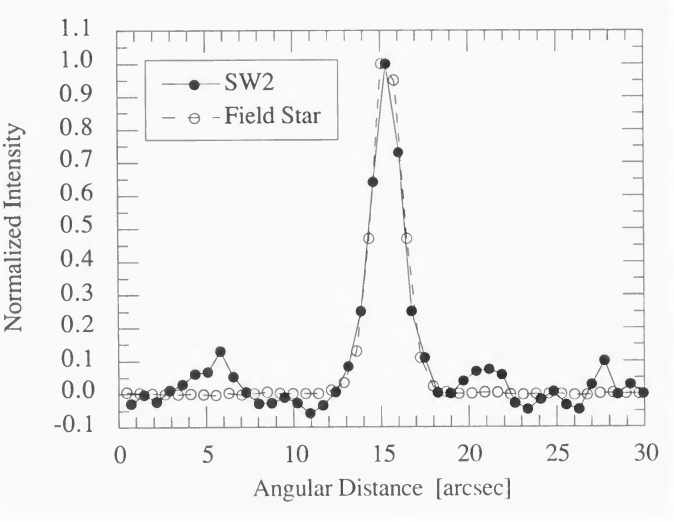

FIG. 5. Surface brightness profiles of SW2 and a field star on UT 1991 15 September. The profile of the comet was obtained by plotting perpendicular to its projected motion. The comet profile is essentially the same as the star, showing no resolved coma.

$$m_{\rm coma}(r) = \Sigma(r) - 2.5\log(2\pi r^2). \quad (3)$$

Equation (3) gives $m_{\rm coma}$ (2.2″) = 23.6 mag, or ~10% of the observed central integrated brightness. We can thus conclude that, even if cometary activity was present at the time of observation, the nucleus still dominated the optical signal in the central 2.2 arcsec radius. This is an *upper limit* to the coma contamination, since the observed coma is not symmetric.

3.3 Nucleus Cross Section

From the mean magnitude of SW2, it is possible to estimate the mean optical cross section of the nucleus. This was done using the equation

$$p_R\bar{C} = \frac{2.25\times 10^{22}\pi R^2\Delta^2 10^{0.4(m_{\rm Sun}-\overline{m_R})}}{10^{-0.4\alpha\beta}} \quad (4)$$

(Eddington 1910), where p_R is the red geometric albedo, $\bar{C}$ [m^2] is the mean cross section, $m_{\rm Sun} = -27.26$ is the R magnitude of the Sun, and $\overline{m_R} = 21.05 \pm 0.05$ is the mean R magnitude of the comet. Assuming $\beta = 0.04$, Eq. (4) yields

$$p_R\bar{C} = 1.2 \pm 0.1 \text{ km}^2 \quad (5)$$

for the product of the albedo with the optical cross section at middle light.

From the profile of SW2, we found that there was very little coma at the time of observation. Our belief that the lightcurve was caused by the nucleus rather than the coma (see Sec. *3.2*) is bolstered by the stellar profile of SW2 and by the following evidence. The rotational phase plot (Fig. 2) shows two asymmetric maxima separated by a steep rise in brightness (at phase ~0.5) to maximum light (~20.8 mag). After the sudden rise, the comet drops to minimum light (~21.3 mag) in 0.8 hrs. If the brightness increase were caused by solid grains in a coma, then the rapid fading would require that the grains moved out of the photometry aperture (2.2 arcsec or 5900 km in radius) at the speed ~2 km/s. Such a speed is nearly an order of magnitude greater than the Bobrovnikoff–Delsemme speed $v_{\rm BD}$ (Delsemme 1982) for this heliocentric distance

$$v_{\rm BD} \sim 580R^{-0.5} = 271 \text{ m/s}.$$

The Bobrovnikoff–Delsemme speed is a molecular outflow speed and thus provides a robust upper limit to the grain speed. Therefore it is likely that the cyclic photometric variations in SW2 are directly due to rotation of an aspherical nucleus, rather than to variations in the amount of near-nucleus coma. In this sense, SW2 may be analogous to P/Tempel 2, in which the observed photometric variations were due to the aspherical nucleus, and the coma brightness was demonstrably constant (A'Hearn *et al.* 1989; Jewitt & Luu 1989).

Since the photometry was dominated by the nucleus, we can infer some optical characteristics of the nucleus. The geometric albedo of the nucleus of SW2 is not known. If we assume a 4% albedo (typical of other known nuclei, see e.g., A'Hearn *et al.* 1989; Millis *et al.* 1988), we find $\bar{C} = 30$ km^2 (at middle light), corresponding to an effective circular radius $r_e = 3.1$ km. More extreme albedos such as 0.02 and 0.10 would yield $r_e = 4.4$ and 2.0 km, respectively. With the presence of coma, these values become upper limits to the radius, and an upper limit of $r_e \leqslant 3.1$ km would render SW2 one of the smallest nuclei yet studied. In particular, Neujmin 1 ($r_e \sim 10$ km), Arend–Rigaux, Halley, and Tempel 2 ($r_e \sim 5$ km) are all larger, while Encke ($r_e \sim 3.5$ km) may be similar in size (Jewitt 1991; A'Hearn 1988, and references therein). We note that our measurement is in disagreement with that by Roemer (1966) who, based on photographic data, reported the cross section of SW2 to be $p\bar{C} = 4.1$ km^2—a cross section nearly four times larger than our result in Eq. (5). Presumably, this disagreement results from the difficulty in photographic photometry of objects near the plate limit, combined with a possibly larger coma contribution. Roemer also made no mention of rotational modulation of the light as reported in the present work. This may partially be explained by strong coma light which obscures the nucleus rotation: Roemer's observations were made when SW2 was closer to the Sun than in the present observations. Another possible factor may be the long integration time: the photographic observations of Roemer required an integration time of ~1 h (Roemer *et al.* 1966), nearly $\frac{1}{5}$ of the entire rotation period. Such a long integration time would average the faint and bright parts of the lightcurve, effectively hiding the rotational variations.

The axis ratio of the nucleus can be estimated from the lightcurve amplitude. Let the perpendicular axes of the nucleus be represented by a, b, and c, with a and b in the equatorial plane. The lightcurve range Δm (~0.5) then is indicative of the ratio of the maximum projection ac and the minimum projection bc, yielding the axis ratio a:b:

$$a{:}b = 10^{0.4\Delta m} = 1.6{:}1. \quad (6)$$

As we may not have observed the equatorial projection of the comet, this axis ratio is only a lower limit. The 1.6:1 axis ratio is thus the minimum asphericity for the nucleus of SW2, the true shape of the nucleus may be even more extreme. The axis ratio for SW2 proves that, like other nuclei, the nucleus of SW2 is elongated (see Table 1 of Jewitt 1991).

3.4 Nucleus Density

Knowledge of the shape and the rotation period of the comet permits the calculation of a lower limit to the nucleus density, assuming it has no significant cohesive strength; this is the minimum density the nucleus must have in order to be stable against centripetal disruption. Equally, it may be viewed as the minimum density of the nucleus required to gravitationally retain a surface regolith or mantle. We can derive this density by setting the centripetal acceleration $(2\pi/P)^2 a$ equal to the gravitational acceleration g:

$$g = (2\pi/P)^2 a. \quad (7)$$

At the apex of a prolate spheroid, the gravitational acceleration is

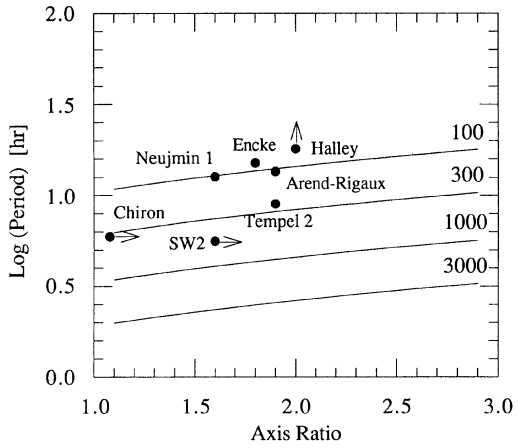

FIG. 6. Logarithm of rotation period vs axis ratio for known comet nuclei. Data are taken from Jewitt & Meech (1988) (Arend–Rigaux, Neujmin 1, Halley); Jewitt & Luu (1989) (Tempel 2); Luu & Jewitt (1990a) (Encke); Luu & Jewitt (1990b) (2060 Chiron). The solid lines show the critical rotation period for prolate spheroid nuclei with densities 100, 300, 1000, and 3000 kg m^{-3}.

$$g=-2\pi G\rho a\int_0^2\left\{\left[1-f^2+\frac{2f^2}{s}\right]^{-1/2}-1\right\}ds, \qquad (8)$$

where $G=6.67\times10^{-11}$ N kg^{-2} m^2 is the gravitational constant, ρ [kg m^{-3}] is the density of the spheroid, a [m] is the spheroid semimajor axis, $f=b/a$ is the ratio of the semiminor axis to the semimajor axis, and s is the distance along the semimajor axis in increments of a (Jewitt & Meech 1988). Integrating Eq. (8), we obtain

$$g=-2\pi G\rho a \times\frac{2f^2(1-f^2)^{1/2}+f^2\ln f^2-f^2\ln(2+2\sqrt{1-f^2}-f^2)}{(1-f^2)^{3/2}}. \qquad (9)$$

Substituting $f=0.625$ and $P=5.58$ h into Eqs. (7) and (9), we find that the critical density of SW2 (assuming a prolate spheroidal shape) is

$$\rho\geqslant460 \text{ kg m}^{-3},$$

if the comet is not to be in a state of internal tensile stress. If the asphericity of the nucleus of SW2 is greater than 1.6:1, this would correspond to a smaller value of f and a smaller g in Eq. (8), hence the net effect is to *increase* the critical density. We conclude that the derived density is a robust lower limit to the density of a strengthless nucleus in SW2.

We note that this lower limit is significantly larger than that derived for comet P/Tempel 2 ($\rho\geqslant300$ kg m^{-3}, Jewitt & Luu 1989), and is also larger than the density of light terrestrial snow ($\rho_{\text{snow}}\sim100$ kg m^{-3}, Perla & Glenne 1981). A large contributor to the high density limit is the small rotation period (the 5.58 h period is the shortest one measured thus far for a comet). In Fig. 6, we compare SW2 with other known nuclei by plotting the period versus the axis ratio for these comets, analogous to Fig. 7 of Jewitt & Meech (1988). Our figure improves upon the latter work by including new data points for SW2, P/Encke, P/Tempel 2, and 2060 Chiron. The figure shows that the densities of comet nuclei are still poorly constrained: the clustering of lower limits near 100 kg m^{-3} implies little about the composition and structure of the nucleus. However, if the nucleus densities are truly as small as these lower limits, then most of the nuclei are in a state of internal stress and are rotating near the critical frequency where centripetal disruption is possible and where gravitationally bound mantles (Rickman *et al.* 1990) may be unable to grow. With a lower limit of 460 kg m^{-3}, SW2 introduces the strictest lower limit so far for the density of a comet nucleus.

3.5 Evolution of Comet SW2

Marsden *et al.* (1973) argued that the nongravitational acceleration of a comet must be inversely proportional to the radius of the nucleus. However, Yeomans & Chodas (1989) recently cautioned against the interpretation of nongravitational parameters in terms of the physical nature of comets, since these parameters can be highly model-dependent for some comets, particularly those having lightcurves which are asymmetric with respect to perihelion. It is not known whether SW2 is best described by the standard nongravitational model or by the asymmetric model, as there is no long-term lightcurve available for SW2. The sample size of known comet nuclei is far from sufficient to test the connection between nucleus size and nongravitational acceleration. However, it appears that, in the case of SW2, the evidence is consistent with the standard nongravitational model: the large A_2 of SW2 is indeed accompanied by a small nucleus size.

The presence of coma in SW2 at the heliocentric distance $R=4.6$ AU may be explained by its recent orbital evolution. Shortly before the discovery of SW2 in 1929, its perihelion distance q was reduced by a Jovian perturbation, from 3.6 to 2.1 AU (Marsden 1969; Marsden *et al.* 1973). The latest calculation of the nongravitational parameters for SW2 (using the standard nongravitational model) showed that A_2 has been growing steadily more negative, implying that q has been slowly decreasing (i.e., the comet orbit is slowly diffusing inward toward the Sun); the decrease in q is attributed to recent further perturbations by Jupiter (Forti 1983). Rickman *et al.* (1991) found that comets which have recently undergone large reductions of q (i.e., which have not had time to make >15 close approaches to the Sun) are associated with large values of A_2. This association led Rickman *et al.* to the conclusion that comets new to the inner solar system have relatively larger free sublimating areas on their surfaces, compared to their precursors. Rickman *et al.* (1990) also found from numerical models that mantles form less easily on small comets than on larger ones, allowing the possibility that the volatile contents of small comets may be exhausted by the time their orbits random-walk into Earth-crossing orbits. They thus predicted that, at large perihelion distances, we would

expect to find large, inactive nuclei and young, active nuclei. We note that comet SW2 fits in very well with this scenario: it is one of the smaller nuclei yet studied, its perihelion distance is large, and it exhibits weak cometary activity even when near aphelion. The large A_2 and the presence of cometary activity at $R \geqslant 4$ AU (albeit weak) are consistent with a relatively large sublimating surface area. Following the hypothesis of Rickman *et al.*, we expect slow mantle growth on SW2, allowing the comet to continuously sublimate. The comet will eventually exhaust its near-surface volatiles, be ejected from the inner solar system or collide with a planet. This scenario predicts persistent activity throughout the orbit of SW2 until volatile exhaustion or ejection.

4. CONCLUSIONS

From photometry of SW2 obtained in September 1991, we conclude the following.

(1) Comet SW2 was detected near aphelion, where it showed a mean R magnitude $\overline{m_R} = 21.05 \pm 0.06$ mag, corresponding to the absolute magnitude m_R (1, 1,0) = 14.64 $\pm$0.06 mag. The lightcurve of SW2 obtained over three separate nights showed nonrandom variations, suggesting a rotating aspherical nucleus. The variations in the photometry are consistent with a period of 5.58 $\pm$ 0.03 h. This is the shortest rotation period measured thus far for a comet.

(2) The comet appeared stellar in individual 360 s integrations. When individual frames are added together (producing an image with a 4.8 h effective integration), the resulting image shows a very faint coma extension, at position angle $\sim 270° \pm 5°$. However, the surface brightness profile of SW2 showed no resolved coma in the direction perpendicular to the projected motion. The extension could be explained by co-moving grains in the orbital plane of the comet which had been ejected earlier from the nucleus; the co-moving grain scenario would eliminate the need for cometary activity at the time of observation. The upper limit to the coma contamination is $\leqslant 10\%$ of the nucleus cross section.

(3) The product of the red geometric albedo with the cross section of the comet at middle light is 1.2 ± 0.1 km^2. Assuming an albedo of 4%, the effective circular radius of SW2 is 3.1 km. With the presence of coma, this represents an upper limit to the radius of the nucleus, rendering SW2 one of the smallest in the sample of known comet nuclei. The small size is consistent with the large transverse nongravitational parameter A_2.

(4) The presence of coma in SW2 near aphelion is consistent with the recent decrease in the perihelion distance of SW2 (~ 10 revolutions ago) and would imply that a relatively large area of fresh sublimating ice is exposed to the Sun.

(5) A strengthless, prolate spheroidal nucleus with the shape and spin period of SW2 would need to have bulk density $\rho \geqslant 460$ kg m^{-3} in order to resist centripetal disruption.

Note added in proof: We recently learned from A'Hearn (1992) that two observations of SW2 in 1981 (near aphelion, $R = 2.20$ and 2.14) yielded a water production rate of 10^{28} s^{-1}, implying an active area of 10^7 m^2. Assuming a 3.1 km radius for SW2, the corresponding fractional active area is $\sim 10\%$—large compared to the fractional active areas of most other known comet nuclei (see Jewitt 1991), and consistent with the scenario described in Sec. *3.5*.

J.L. thanks Paul Schechter for the allocation of time at the MDM Observatories, the helpful staff at MDM Observatories, and B. Marsden for helpful discussion. We thank R. Millis for helpful comments on the manuscript. D.J. acknowledges support of this work via a grant from the National Science Foundation, and J.L. acknowledges the support of the Smithsonian Institution through a Harvard–Smithsonian Fellowship.

REFERENCES

A'Hearn, M. F. 1988, Ann. Rev. Earth Planet. Sci., 16, 273
A'Hearn, M. F. 1992, private communication
A'Hearn, M. F., Campins, H., Schleicher, D. G., & Millis, R. L. 1989, ApJ, 347, 1155
Belton, M. J. 1991, in Comets in the Post-Halley Era, edited by R. L. Newburn, Jr., M. Neugebauer, and J. Rahe (Kluwer, Dordrecht), pp. 691–712
Bortle, J. 1979, Periodic Comet Schwassmann–Wachmann 2 (1979k), IAU Circular 3575
Carusi, A., Kresák, L., Perozzi, E., & Valsecchi, G. B. 1985, Long-Term Evolution of Short-Period Comets (Adam Hilger, Ltd., Bristol)
Christian, C. A., Adams, M., Barnes, J. V., Butcher, H., Hayes, D. S., Mould, J. R., & Siegel, M. 1985, PASP, 97, 363
Delsemme, A. H. 1982, in Comets, edited by L. L. Wilkening (University of Arizona Press, Tucson), pp. 85–130
Dworetsky, M. M. 1983, MNRAS, 203, 917
Eddington, A. S. 1910, MNRAS, 70, 442
Forti, G. 1983, A&A, 215, 381
Jewitt, D. C. 1991, in Comets in the Post-Halley Era, edited by R. L. Newburn, Jr., M. Neugebauer, and J. Rahe (Kluwer, Dordrecht), pp. 19–66
Jewitt, D., & Luu, J. 1989, AJ, 97, 1766
Jewitt, D., & Meech, K. 1988, ApJ, 328, 974
Luu, J., & Jewitt, D. 1990a, Icarus, 86, 69
Luu, J., & Jewitt, D. 1990b, AJ, 100, 933
Marsden, B. G. 1969, AJ, 74, 720
Marsden, B. G., Sekanina, Z., & Yeomans, D. K. 1973, AJ, 78, 211
Millis, R. L., A'Hearn, M. F., & Campins, H. 1988, ApJ, 324, 1194
Perla, R., & Glenne, B. 1981, in Handbook of Snow, edited by D. M. Gray and D. H. Male (Pergamon, Toronto), pp. 709–740
Rickman, H., Fernandez, J. A., & Gustafson, B. Å. S. 1990, A&A 237, 524
Rickman, H., Froeschlé, C., Kamél, L., & Festou, M. C. 1991, AJ, 102, 1446
Roemer, E. 1966, Mem. Soc. Roy. Sci. Liège XII, 23–28
Roemer, E., Thomas, M., & Lloyd, R. E. 1966, AJ, 71, 591
Sekanina, Z. 1976, in The Study of Comets, edited by B. Donn, M. Mumma, W. Jackson, M. A'Hearn, and R. Harrington, NASA SP-393, (U. S. Government Printing Office, Washington, DC), pp. 537–587
Yeomans, D. K., & Chodas, P. W. 1989, AJ, 98, 1083

THE ASTRONOMICAL JOURNAL

FOUNDED BY B. A. GOULD
1849

VOLUME 104 **December 1992 ~ No. 1643** *NUMBER 6*

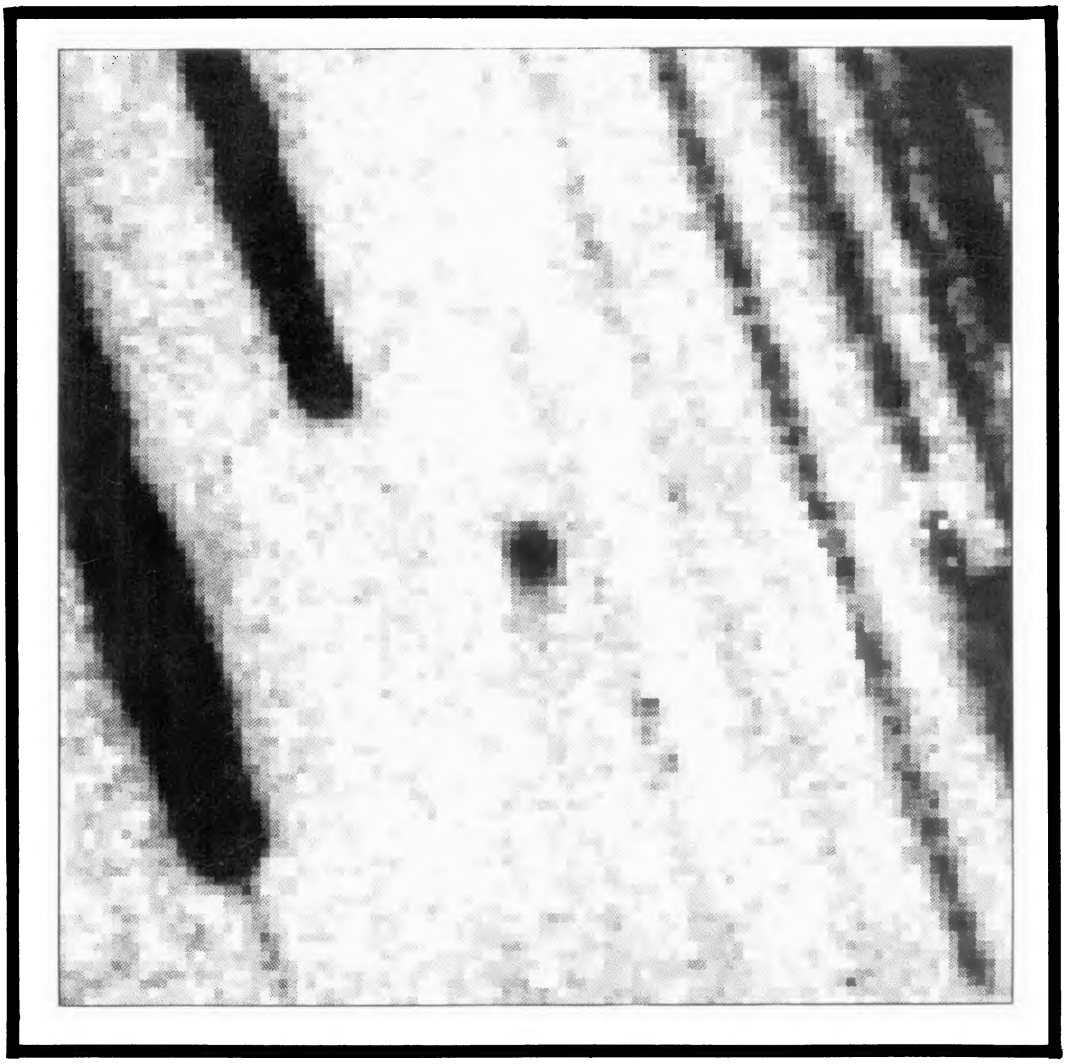

(See Page 2243)

Published for the
AMERICAN ASTRONOMICAL SOCIETY
by the
AMERICAN INSTITUTE OF PHYSICS